

Options for Control of Reactive Power by Distributed Photovoltaic Generators

This paper presents challenges and opportunities for distribution utilities, simulates options for managing reactive power, and discusses benefits of choosing local variables to control the system.

By KONSTANTIN TURITSYN, Member IEEE, PETR ŠULC,
SCOTT BACKHAUS, AND MICHAEL CHERTKOV

ABSTRACT | High-penetration levels of distributed photovoltaic (PV) generation on an electrical distribution circuit present several challenges and opportunities for distribution utilities. Rapidly varying irradiance conditions may cause voltage sags and swells that cannot be compensated by slowly responding utility equipment resulting in a degradation of power quality. Although not permitted under current standards for interconnection of distributed generation, fast-reacting, VAR-capable PV inverters may provide the necessary reactive power injection or consumption to maintain voltage regulation under difficult transient conditions. As side benefit, the control of reactive power injection at each PV inverter provides an opportunity and a new tool for distribution utilities to optimize the performance of distribution circuits, e.g., by minimizing thermal losses. We discuss and compare via simulation various design options for control systems to manage the reactive power generated by these inverters. An important design decision that weighs on the speed and quality of communica-

tion required is whether the control should be centralized or distributed (i.e., local). In general, we find that local control schemes are able to maintain voltage within acceptable bounds. We consider the benefits of choosing different local variables on which to control and how the control system can be continuously tuned between robust voltage control, suitable for daytime operation when circuit conditions can change rapidly, and loss minimization better suited for nighttime operation.

KEYWORDS | Distributed generation; feeder line; photovoltaic (PV) power generation; power flow; voltage control

I. INTRODUCTION

Displacing fossil-fired generation with renewable generation has many desirable outcomes, e.g., reduction in pollution and CO₂ emissions, and a significant challenge, i.e., reliable delivery of electrical power of acceptable quality nearly 100% of the time [1]. The mix of renewable generation will contain many different resources including wind, concentrating solar power, and photovoltaic (PV) at the transmission-scale, but with PV as the only presently viable option at the distribution scale. The one challenge stated above is actually a family of challenges because each of these renewable options affects reliability and power quality in different and often multiple ways.

At the transmission scale, renewable generation projects are generally large enough to warrant individual transmission interconnection studies intended uncover issues that may need to be mitigated by the renewable generation owner, such as installing certain additional

Manuscript received February 1, 2011; accepted February 11, 2011. Date of current version May 17, 2011. The work of P. Šulc and M. Chertkov was partially supported by NMC via an NSF collaborative Grant CCF-0829945 on "Harnessing Statistical Physics for Computing and Communications." Research at LANL was carried out under the auspices of the National Nuclear Security Administration of the U.S. Department of Energy at Los Alamos National Laboratory under Contract DE C52-06NA25396.

K. Turitsyn is with the CNLS and Theoretical Division, Los Alamos National Lab, Los Alamos, NM 87545 USA (e-mail: turitsyn@lanl.gov).

P. Šulc is with the New Mexico Consortium, Los Alamos, NM 87544 USA. He is also with Czech Technical University in Prague, Czech Republic (e-mail: sulcpetr@gmail.com).

S. Backhaus is with the Materials, Physics and Applications Division, Los Alamos National Lab, Los Alamos, NM 87545 USA (e-mail: backhaus@lanl.gov).

M. Chertkov is with the CNLS and Theoretical Division, Los Alamos National Lab, Los Alamos, NM 87545 USA. He is also with the New Mexico Consortium, Los Alamos, NM 87544 USA (e-mail: chertkov@lanl.gov).

Digital Object Identifier: 10.1109/JPROC.2011.2116750

equipment or operating in certain ways to mitigate the problems. In this case, the cost of mitigation is borne by the generator creating the problem.

At the distribution scale, the size of an individual PV generator is so small that the cost of an “interconnection study” would be prohibitive. However, when the penetration of PV generators on any particular distribution circuit is low, the impact is quite small and present utility systems are generally unaffected. However, at higher penetrations the net impact of many small PV generators may accumulate and affect power quality, e.g., slowly responding utility equipment (tap changers, switchable capacitors, etc.) not keeping pace with cloud-induced rapid variations of PV generation resulting in loss of voltage regulation. Fast-response equipment could be installed to rectify the problem (e.g., a D-STATCOM [2]), but the cost is borne by the entire rate base instead of the owners of the PV generators who are benefiting from the interconnection to the distribution grid.

A potential solution to the voltage regulation problem is to tap into the latent excess PV inverter capacity to generate or consume reactive power to control voltage. Although not permitted by current interconnection standards [3], changes to these standards to allow for injecting or consuming reactive power appear eminent. Under this scheme, the burden of providing adequate reactive power compensation is again placed upon the generator seeking access to the grid. However, many questions still remain including the following:

- How to dispatch the excess capacity to handle major changes in circuit conditions, e.g., rapid change from a net real power export to net real power import?
- How to split the reactive compensation duty equitably between the PV generators?
- Whether the control should be centralized (potentially vulnerable), distributed (perhaps more robust), or a combination of the two?
- Whether centralized or distributed, what variables should be used as inputs to the control algorithm?

Despite the challenges related to accommodating PV generators, there is also an opportunity for the utility to leverage the inverters of these PV generators to enhance its own performance such as improving power quality (i.e., voltage regulation) and reducing distribution losses via optimal management of reactive power flows. However, these should be accomplished without placing undue burdens on the PV generators by either via excessive dispatch of reactive power or by limiting PV generation.

After reviewing traditional reactive dispatch approaches in Section II, we focus in Section III on the issues surrounding the integration of high penetrations PV generation into distribution circuits and their impact on reactive power control systems. In Section V, we review a few control methods that have been proposed and present our own potential control method. Section VI compares these methods via simulations of a distribution circuit under widely varying conditions. We conclude and discuss directions for future work in Section VII.

II. TECHNIQUES OF REACTIVE COMPENSATION

Traditional power systems are designed vertically. Power is generated at large power plants, it is then delivered to consumers via a hierarchical network of transmission and distribution grids. In distribution systems, the voltage is normally controlled only at the entry point (substation), and then it sags down the distribution lines, mainly because of consumption of reactive power by end consumers and the impedance of the distribution lines. A number of technologies are employed in the modern power systems to compensate for the flux of reactive power and thus to improve the power quality in the system. These technologies compensate for the drop of voltage using controlled injections of reactive power at a few locations. In this Section we briefly review some of these existing technologies which are also relevant to our own work discussed in the following sections.

A. Synchronous Generators

Large synchronous generators typically control their output voltage within the prescribed bounds by manipulating (usually injecting) reactive power. Control is realized via an excitation system that consists of an ac or dc exciter, controller and voltage measurement components [4], [5], and this system provides an efficient means to stabilize the high-voltage part of the power grid. However, the application of this system is limited geographically to the entry point to the power distribution system. Reactive power supplied by these generators has thus limited affect on the voltage and reactive power control in the distribution system. For these reasons additional compensating technologies are required to ensure the power quality in the remote parts of the distribution networks.

B. Capacitor Banks

Shunt capacitor banks are usually installed and operated in the distribution networks by local utility companies. The capacitor banks consist of a number of large capacitors that can be connected to, or disconnected from, the system by switches. From the viewpoint of the grid the shunt capacitors act like a source of reactive power. Typically utilities install only a small number of large capacitor banks in special locations of the distribution network. Optimal placement and switching of capacitor banks is recognized as an important and challenging problem in power system design and control. Since the seminal works by Baran and Wu [6]–[8] and Baldick and Wu [9], many approaches have been applied to the problem including genetic algorithms and fuzzy logic (see, e.g., [10], [11]). A recent review of the progress in the field can be found in [12].

Optimal operation of capacitor banks attempts to achieve a balance between the following objectives.

- Improve power quality, and specifically the magnitude of voltage variations. Typical standards

require that the voltage level is stayed within $\approx 5\%$ of deviation from the nominal value.

- Reduce thermal losses in the system. Reactive components of the power flow increase the current amplitude I , and thereby the thermal losses rI^2 . Proper redistribution of the reactive power sources results in local correction of the power factor and reduce losses in the lines.
- Increase system capacity. An increase in power factor allows more real power to be transferred through the system without exceeding capacity limits of the lines.

There are also some down sides in integrating capacitor banks in distribution grids. Switching of a single capacitor produces a strong transient which propagates through the network and may cause a significant damage to equipment. Another potential drawback of capacitor banks is associated with generation of high-frequency harmonics. The resistance–inductance–capacitance (RLC) circuits formed by capacitor banks connected into inductive lines may lead to resonances at some frequencies, where the effects of capacitance and of the inductance are canceled. Harmonic excitations produced by other nonlinear equipment may be amplified resulting in an unacceptable degradation of power quality. Additional harmonic filtering equipment is required to mitigate these dangerous side effects of capacitor banks.

It is also questionable whether the capacitor bank technology is sufficient to answer the challenges associated with distributed renewable generation penetrating to the distribution systems. Whether the capacitor bank installations can alleviate the destabilizing effects of intermittent energy sources remains an open question. Distribution systems with high penetration of distributed renewable generators may require faster and more flexible control systems than achievable with capacitor banks.

C. End-User Reactive Compensation

Inverter-based technologies discussed in this work belong to an emerging class of end-user reactive dispatch technologies which are not yet extensively deployed. However, there are several reasons that make them highly promising as follows.

- *Efficiency.* Proximity of reactive compensation to the reactive load decreases the average magnitude of current flowing through the system and thereby reduces the thermal losses.
- *Flexibility.* Reactive flows generated by distributed compensation systems result from a large number of individual compensators that can combine their reactive injections in multitude of ways, allowing the system to achieve optimal operation.
- *Scalability.* Large-scale capacitor banks constrains the expansion of the distribution systems and require coordination between the capacitor banks upgrades and new renewable generator installa-

tions. Local compensation allows easy and on-the-fly system upgrades.

- *Reliability.* Relying on large capacitor banks makes the grid vulnerable to equipment failure. Moreover, from the cybersecurity viewpoint, a distributed control system with limited communication between its smaller components is potentially more resilient to cyberattacks in comparison to centralized control systems that control larger equipment.

III. OPPORTUNITIES AND CHALLENGES

Fig. 1 introduces the schematic distribution circuit and most of the notation we will use in the remainder of the manuscript. In our previous work [13], [14], we have used the *LinDistFlow* equations [6]–[8] to compute voltage and power flows. In this work, we switch to an ac solver [15] to compute all distribution circuit quantities. However, we introduce the problem using the *LinDistFlow* equations because they provide an excellent setting for gaining intuition about the competing nature of achieving good power quality, i.e., voltage regulation, and reducing distribution circuit losses. The *LinDistFlow* equations for the circuit in Fig. 1 can be written

$$P_{j+1} = P_j - p_{j+1}^{(c)} + p_{j+1}^{(g)} \quad (1)$$

$$Q_{j+1} = Q_j - q_{j+1}^{(c)} + q_{j+1}^{(g)} \quad (2)$$

$$V_{j+1} = V_j - (r_j P_j + x_j Q_j) / V_0 \quad (3)$$

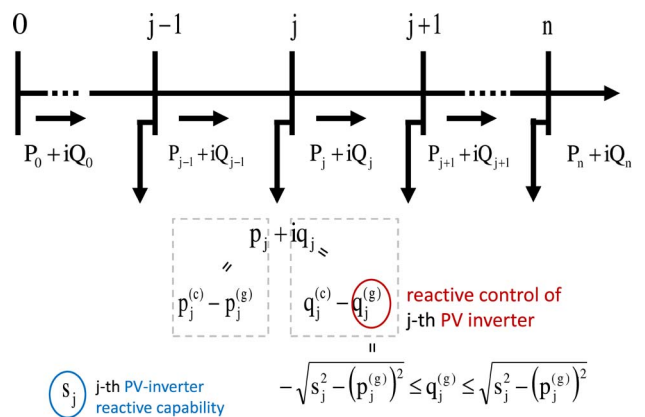


Fig. 1. Diagram and notations for the radial network. P_j and Q_j represent real and reactive power flowing down the circuit from node j , where P_0 and Q_0 represent the power flow from the sub-station. p_j and q_j correspond to the flow of power out of the network at the node j , where the respective positive [negative] contributions, $p_j^{(c)}$ and $q_j^{(c)}$ [$p_j^{(g)}$ and $q_j^{(g)}$] represent consumption [generation] of power at the node. The node-local control parameter $q_j^{(g)}$ can be positive or negative but is bounded in absolute value as described in (4). The apparent power capability of the inverter s_j is preset to a value comparable to but larger than $\max p_j^{(g)}$.

where $P_j + iQ_j$ is the complex power flowing away from node j toward node $j + 1$, V_j is the voltage at node j , $r_j + ix_j$ is the complex impedance of the link between node j and $j + 1$, and $p_j + iq_j$ is the complex power extracted at node j . Both p_j and q_j are composed of local consumption minus local generation due to the PV inverter, i.e., $p_j = p_j^{(c)} - p_j^{(g)}$ and $q_j = q_j^{(c)} - q_j^{(g)}$. Of the four contributions to $p_j + iq_j$, $p_j^{(c)}$, $p_j^{(g)}$ and, $q_j^{(c)}$ are uncontrolled (i.e., driven by consumer load and instantaneous PV generation), while the reactive power generated by the PV inverter, $q_j^{(g)}$, can be adjusted and be made either positive or negative. As described in Section V, $q_j^{(g)}$ is limited by the apparent power capability of the inverter s_j

$$\forall j = 1, \dots, n : \quad |q_j^{(g)}| \leq \sqrt{s_j^2 - (p_j^{(g)})^2} \equiv q_j^{\max}. \quad (4)$$

Note that reactive power generation is possible only at the nodes with PV generation. For the other nodes, we take $s_j = p_j^{(g)} = q_j^{(g)} = 0$.

Within the framework of *LinDistFlow* equations, the rate of energy dissipation \mathcal{L}_j and the change in voltage ΔV_j between nodes j and $j + 1$ of the distribution circuit are given by

$$\mathcal{L}_j = r_j \frac{p_j^2 + Q_j^2}{V_0^2} \quad (5)$$

$$\Delta V_j = -(r_j P_j + x_j Q_j) / V_0. \quad (6)$$

A. Distribution Loss Reduction vs Power Quality

Equations (5) and (6) can be used to discuss many of the issues surrounding how to construct a control scheme to use the latent reactive power capability of PV inverters to maintain power quality and reduce losses. First, (5) shows that losses in any circuit segment j are minimized when $Q_j = 0$. However, to minimize the voltage variation, (6) would prefer if $Q_j = -(r_j/x_j)P_j$ in clear competition with loss minimization. Therefore, in general, we should not expect a control algorithm to simultaneously provide optimal voltage regulation and minimize losses. The trade between these two desired outcomes must be left up to engineering judgement. However, a control scheme should be adaptable to easily allow for smooth transitions between emphasis on power quality or distribution losses.

Equation (6) also demonstrates the importance of controlling $q_j^{(g)}$ in a high PV penetration distribution circuit. As irradiance conditions change due to cloud passage and the $p_j^{(g)}$ change rapidly, the segment flows P_j can undergo rapid reversals. A distribution circuit that was experiencing an acceptable 0.05 p.u. voltage drop without PV generation could see rapid switching between the original voltage drop and a 0.05 p.u. voltage rise

potentially causing voltage excursions beyond acceptable bounds. However, if the Q_j can also be rapidly modified through the $q_j^{(g)}$, then the voltage variation can be controlled to within acceptable bounds.

B. Centralized Versus Local Control

Equations (5) and (6) also demonstrate the complexity of developing a centralized control scheme versus local control. The losses and voltage drop in circuit segment j depend upon the flows in segment j , i.e., P_j and Q_j . Although not currently available to utilities, a centralized controller could infer the flows in each segment from smart meter data that provides q_j and p_j for each consumer. With P_j and Q_j , a centralized controller could determine the dispatch of $q_j^{(g)}$ by optimizing an objective function that includes weighted measures of losses and voltage deviations. For this type of centralized control, the communication requirements and additional system vulnerability due to reliance on communication may outweigh the potential performance benefits. In addition, latency in communication and control may degrade performance during rapid changes in cloud cover.

Local control schemes that act on local variables will not suffer from latency and are much less vulnerable as they do not depend upon communication for their operation (limited communication may be employed by a utility to change control algorithms perhaps up to several times during the day as overall circuit conditions change [16]). However, truly local schemes will only have access to local flows p_j and q_j and, without access to the segment flows P_j and Q_j , cannot guarantee optimal control. This suggests a local scheme must rely upon heuristics to infer enough information about P_j and Q_j to take appropriate control actions.

In recent work, [13] we have compared centralized and local approaches to the control of reactive power. We have shown that, for a realistic distribution circuit, a local control scheme that simply supplies the local reactive power consumption (i.e., $q_j^{(g)} = q_j^{(c)}$) can achieve almost 80% of savings in losses when compared to a centralized control based on solving the full optimization problem. Losses were actually reduced farther by blending in another heuristic to infer P_j and Q_j to reduce voltage drops [14]. The additional heuristic works well in reasonably high PV penetration scenarios when the circuit is importing or exporting power. However, when PV generation and load on the circuit are in relatively close balance, the heuristic breaks down and may actually result in reduced performance. Although, when a circuit is in balance, the P_j randomly change sign from segment to segment, and the need to dispatch $q_j^{(g)}$ to regulate voltage is not high. Considering the advantages in speed and reliability of local versus centralized control and the comparable performance we have simulated in previous work [13], [14], we only consider local control in the remainder of this manuscript.

C. Equitable Treatment of PV Generators

Dispatching $q_j^{(g)}$ places additional duty on the inverters of individual PV generators which may lead to reduced lifetime and increased lifecycle cost. Reference [16] seeks to equitably divide the reactive power duty by setting the maximum positive and negative $q_j^{(g)}$ dispatch proportional to the capacity of the inverter and PV generator. However, the variable that controls $q_j^{(g)}$ between these two extremes is the local voltage V_j . Therefore, PV generators that are located on a distribution circuit where the voltage is continually above or below 1 p.u. will have to endure extra duty compared to those located where the voltage is usually close to 1 p.u. Retail customers typically have no choice where they are located along a circuit. In addition, their location relative to a substation may change from day to day depending on how the entire distribution system is configured. Therefore, customers should not be penalized based on this location. In one of the alternative control schemes presented in this manuscript, we base control of $q_j^{(g)}$ solely on $p_j^{(c)}$, $p_j^{(g)}$, and $q_j^{(c)}$ with reactive power limits set by the capacity of the inverter so that $q_j^{(g)}$ does not depend on location along a circuit.

In this manuscript, we only discuss the dispatch of reactive power and do not consider the calls for limiting PV generation. Although we have not encountered situations where this control action is required, [16] provides a framework for an equitable division of generation reductions.

IV. MODELING DETAILS

A. Inverter Model

An inverter attached to a PV generator is not an infinite source or sink of reactive power. Its instantaneous reactive power capability is limited by its fixed apparent power capability s_j and the variable real power generation $p_j^{(g)}$. To describe this limitation mathematically, we adopt a model of PV inverters previously described in [13] and [17] where the range of allowable reactive power generation is given by $|q^{(g)}| \leq \sqrt{s^2 - (p^{(g)})^2} \equiv q^{\max}$. This relationship is also described by the phasor diagram in Fig. 2. When s is larger than $p^{(g)}$, the inverter can supply or consume reactive power $q^{(g)}$. The inverter can dispatch $q^{(g)}$ quickly (on the cycle-to-cycle time scale) providing a mechanism for rapid voltage regulation. As the output of the PV panel array $p^{(g)}$ approaches s , the range of available $q^{(g)}$ decreases to zero. On a clear day with the sun angle aligned with the PV array, $p^{(g)} = p_{\max}^{(g)}$ and the range of available $q^{(g)}$ is at a minimum. Although s_j relative to $p_{\max}^{(g)}$ could be treated as a free parameter subject to optimization, our previous work [13] found that $s_j \approx 1.1p_{\max}^{(g)}$ provides enough freedom in $q_j^{(g)}$ to realize the majority of the reduction in distribution losses. Under these conditions, $|q_j^{(g)}| \leq 0.45p_{\max}^{(g)}$ when $p_j^{(g)} = p_{\max}^{(g)}$. The choice of $s_j \approx 1.1p_{\max}^{(g)}$ seems reasonable because inverters are available in discrete sizes and inverters are likely oversized somewhat compared to $p_{\max}^{(g)}$.

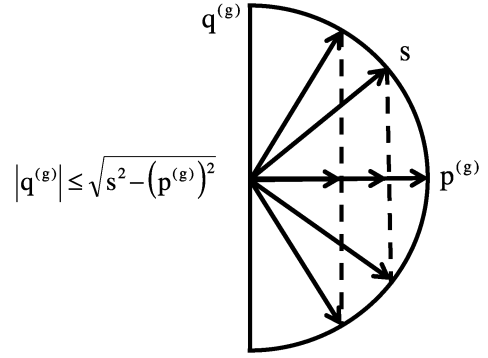


Fig. 2. Inverter capability model.

B. Description of the Prototypical Distribution Circuit

The configuration of the distribution circuit model we consider is similar to one we previously used [13], [14]. Many of the circuit parameters are based on one of the 24 prototypical distribution circuits described in [18]; the nominal phase-to-neutral voltage V_0 is 7.2 kV, line impedance is $(0.33 + 0.38i) \Omega/\text{km}$ and constant along the circuit, and the distance between neighboring nodes is 0.2 km. The circuit consists of 250 nodes, and we study one level of PV penetration, i.e., 50% of the nodes include PV generation. The capacity of the inverter at each PV-enabled node is set to $s_j = 2.2$ kVA, and the maximum generation capacity is set to $p_{\max}^{(g)} = 2.0$ kW. Uniform level of maximum PV power generation assumes identical installations at each PV-enabled node (the same $p_{\max}^{(g)}$ installed in the same way) and spatially uniform solar irradiance.

We consider two different load/generation cases; undergenerated and overgenerated. The undergenerated case corresponds to a situation when there is heavy cloud cover over the entire circuit and all of the $p_j^{(g)} = 0$. The load at each node is selected from a uniform distribution between 0 and 2.5 kW giving an average net real power import per node of 1.25 kW. The overgenerated case corresponds to a clear sky where all $p_j^{(g)} = 2$ kW. The load at each node is again selected from a uniform distribution, but the limits are now 0 and 1 kW. The average generation per node is then 1 kW and the average load per node is 0.5 kW giving an average net real power export per node of 500 W. The reactive power consumed by the loads at each node, $q_j^{(c)}$, is randomly selected from uniform distribution between $0.2p_j^{(c)}$ and $0.3p_j^{(c)}$ corresponding power factors in the range from 0.955 to 0.98, which is representative of residential loading [19].

The two cases we consider correspond to widely varying irradiance and power flow conditions. For a given control scheme, the differences between these cases probes the robustness of the scheme to rapidly changing irradiance conditions. To gauge the sensitivity of the control schemes considered in the manuscript to changes in circuit

configurations, we consider many different realizations of the circuit. In each realization, the 50% of the nodes that are PV-enabled are selected randomly and the $p_j^{(c)}$ and $q_j^{(c)}$ distributions are sampled each time.

C. Power Flow Solution Method

We use the Matpower package [15] to solve the ac power flow equations. The package implements the Newton-Raphson method to solve the equations

$$0 = -(p_i^c - p_i^g) + \sum_{k=1}^N |V_i||V_k|(G_{ik} \cos \theta_{ik} + B_{ik} \sin \theta_{ik}) \quad (7)$$

$$0 = -(q_i^c - q_i^g) + \sum_{k=1}^N |V_i||V_k|(G_{ik} \sin \theta_{ik} - B_{ik} \cos \theta_{ik}) \quad (8)$$

where G_{ik} and B_{ik} are the real and imaginary parts of the impedance matrix Y , respectively, and θ_{ik} is the difference in voltage phase angle between buses i and k .

The Matpower package solver does not support situations where $q_i^{(g)}$ becomes a function of voltage. For the control schemes that require this (described below), we modify the implementation of the Newton-Raphson method to take into account the variation of $q_i^{(g)}$ with respect to the voltage.

V. CONTROL SCHEMES

A. Control on Local Voltage Only

Seal (2010) [16] has proposed a reasonable framework for local control of reactive power produced by the inverters of PV generators. Although four different modes of control are proposed, each consists of a set of piecewise linear relationships between $q_j^{(g)}$ and V_j . A simplified version of mode ‘‘PV1’’ from [16] is shown in Fig. 3. Although not specified in [16], we take $q_j^{(g)} = 0$ at $V_j = 1$ p.u., and we take the saturated values of $q_j^{(g)}$ at high and low values of V_j to be given

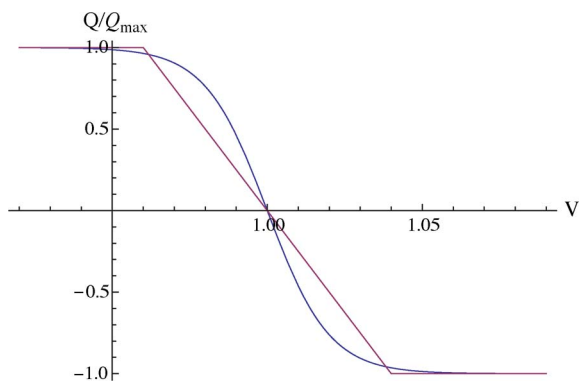


Fig. 3. Voltage control curves proposed in [16] and employed in (9).

by q_j^{\max} defined in the earlier discussion of the inverter model. Except for the dynamic definitions of q_j^{\max} , this is essentially a proportional control scheme where $q_j^{(g)}$ depends linearly on V_j .

In our attempts to utilize this scheme, the Matpower ac solver [15] we employed showed convergence problems which we diagnosed as the solution jumping back and forth across the points of discontinuous first derivative in the control function. To ease this difficulty, we smoothed the control function in Fig. 3 using a sigmoid function, i.e.,

$$G(q_j^{\max}, V_j, \delta) = q_j^{\max} \left(1 - \frac{2}{1 + \exp[-4(V_j - 1)/\delta]} \right). \quad (9)$$

Here, δ is simply a parameter that controls how closely the smoothed control function approximates the sharp transitions of the original control function. In this work we have taken $\delta = 0.04$, and $G(q_j^{\max}, V, 0.04)$ is plotted as the dark red curve in Fig. 3 for comparison to the piecewise continuous control proposed in [16].

B. Control on Local Flows Only

The control function $G(q_j^{\max}, V, \delta)$ describes a form of local control that only depends on the voltage at the point of inverter connection. Since this voltage is immediately available to the inverter, G describes a scheme that would be very convenient to implement. However, if the predicted replacement of mechanical meters with smart meters occurs, information in addition to voltage may be available to control an inverter’s $q_j^{(g)}$. We assume a smart meter will be able to provide both real and reactive net power flows and that these can be communicated to the local PV inverter. The inverter will already have measures of its own real and reactive power generation. The combination of this data will easily provide the inverter with near real-time access to the three local, uncontrolled power flows, i.e., $p_j^{(c)}$, $q_j^{(c)}$, and $p_j^{(g)}$. It is from these local power flows, as opposed to V_j , that we construct an alternative control scheme. We could also explicitly include V_j , however, as discussed earlier, this choice could easily lead to inequities based upon where a PV generator is located along a distribution circuit.

In previous work [14], we have analyzed control schemes of the general form

$$q_j^{(g)} = F_k(p_j^{(g)}, p_j^{(c)}, q_j^{(c)}) \quad (10)$$

and consistent with constraint (4). Here, we summarize some of that work. The control scheme is local in that $q_j^{(g)}$ depends only on $p_j^{(g)}, p_j^{(c)}, q_j^{(c)}$. Similar to the voltage scheme discussed above, we also assume that the control is homogeneous over the line: all inverters are programmed

in the same way, and explicit dependence on the bus number j enters through the inverter's dynamically determined capability q_j^{\max} which in turn depends on s_j and $p_j^{(g)}$ through (4).

It is useful to introduce the following “helper” function, $\text{Constr}_j[q]$, meant to enforce the constraint (4)

$$\text{Constr}_j[q] = \begin{cases} q, & |q| \leq q_j^{\max} \\ (q/|q|)q_j^{\max}, & \text{otherwise.} \end{cases} \quad (11)$$

A local control scheme proposed in [13] was based on the heuristic that losses are minimized when the reactive flows Q_k are zero, and the $q_j^{(g)}$ were chosen to minimize the net reactive power consumption $q_j^{(c)} - q_j^{(g)}$ at each node

$$F_k^{(L)} = \text{Constr}_k[q_k^{(c)}]. \quad (12)$$

In this scheme, the inverter supplies the local consumption of reactive power up to the limits imposed by its capacity s_j and generation $p_j^{(g)}$. This scheme was shown to be very effective in reducing the losses. However, as discussed in Section III, loss minimization and voltage regulation are competing objectives and minimizing losses does not ensure voltage regulation.

In [14], the control in (12) was extended to consider voltage regulation. Equation (3) suggests that, to reduce variations in V_j , we should minimize the absolute value of the combined power flow $r_j P_j + x_j Q_j$. Note that for many circuits, the ratio of $r_j/x_j = \alpha$ is nearly constant for all k and depends only on the configuration and size of the conductors used. Thus the absolute value of $r_j P_j + x_j Q_j$ will be exactly zero if for every load node we ensure that $p_j^{(c)} - p_j^{(g)} + \alpha(q_j^{(c)} - q_j^{(g)}) = 0$ suggesting a control function $F_j^{(V)}$ aimed at minimizing voltage variations without regard for losses

$$F_j^{(V)} = \text{Constr}_k \left[q_j^{(c)} + \frac{p_j^{(c)} - p_j^{(g)}}{\alpha} \right]. \quad (13)$$

The control in (12) seeks to minimize losses while the control defined in (13) seeks to regulate voltage. A continuous compromise between the two objectives in can be achieved via the following nonlinear combination:

$$F_j(K) = \text{Constr}_k \left[K F_j^{(L)} + (1 - K) F_j^{(V)} \right] \quad (14)$$

where K is a single parameter controlling the trade off between the two objectives in (11). At $K = 1$ we recover the loss reduction scheme of (12), whereas at $K = 0$ we recover

the voltage regulation scheme of (13). Through the parameter K , we now have a simple method to smoothly adapt the control scheme, if necessary, as circuit conditions change.

C. Hybrid Control

We have argued that inclusion of V_j as an input to the control method may result in inequitable division of reactive power generation duty. However, heuristics used to create the control in (14) may, under certain circumstances, fail to provide a good estimate of the segment flows P_j and Q_j . Without knowledge of V_j , the control in (14) has no way of correcting if V_j has moved significantly from 1 p.u. To correct this shortcoming, we create a hybrid control that combines (9) and (14).

The concept behind the hybrid control is similar to that used in blend $F_j^{(L)}$ and $F_j^{(V)}$ in (14). We desire that if $V_j = 1$ p.u., then the control of $q_j^{(g)}$ is completely governed by (14). However, if V_j has fallen significantly below 1 p.u., then $q_j^{(g)} \rightarrow q_j^{\max}$. Similarly, if V_j has risen significantly above 1 p.u., then $q_j^{(g)} \rightarrow -q_j^{\max}$. A simple control that achieves this behavior is given by

$$H_j(K, V_j) = F_j(K) + G \left(q_j^{\max} - F_j(K), V_j, \delta \right). \quad (15)$$

At $V_j = 1$, $G = 0$ and $H_j = F_j$. For $V_j \ll 1$, $G \rightarrow q_j^{\max} - F_j(K)$ and $H_j \rightarrow q_j^{\max}$. Finally, if $V_j \gg 1$, $G \rightarrow -(q_j^{\max} - F_j(K))$ and $H_j \rightarrow -(q_j^{\max} + 2F_j(K))$ which is still bounded between $\pm q_j^{\max}$. Here, we have chosen to blend the G and F control in one particular way. There are clearly other ways to achieve these, but we leave this for future study.

VI. SIMULATIONS: RESULTS AND DISCUSSIONS

The control schemes described in Section V are simulated on the distribution circuit described in Section IV-B. The node voltages and the distribution circuit losses are calculated for both the under- and overgenerated cases. For the undergenerated case, the node voltages are presented in Fig. 4 and the losses in Fig. 5. For the overgenerated case, the node voltages are presented in Fig. 6 and the losses in Fig. 7.

A. Base Case-No Control With $q_j^{(g)} = 0$

The base case where all $q_j^{(g)} = 0$ corresponds to the situation imposed by the current distributed generation interconnection standards [3]. In the undergenerated case where P_j and Q_j are in the same direction, the voltage deviation below 1 p.u. is quite large at about 0.07 p.u. In the overgenerated case, P_j and Q_j are now in opposite directions for the majority of j and, in spite of not taking any actions, the maximum voltage rise of about 0.015 p.u. is relatively small. In both cases, the maximum deviations take place at or very near to the end of the distribution circuit. However, during

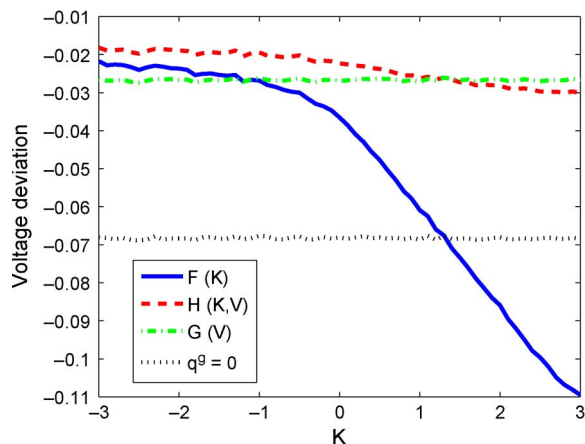


Fig. 4. Undergenerated case: Maximum deviation of V_j from 1 p.u. Black dotted line: No control, $q_j^{(g)} = 0$; green dashed line: control via local voltage, blue solid line: control via local power flows, red dashed line: hybrid control.

partly cloudy daylight hours, the voltage will swing 0.085 p.u. as the circuit transitions between the under and over-generated cases we consider—uncomfortably close to allowable limits. Under higher load or PV generation conditions, the voltage swings would easily exceed 0.1 p.u. demonstrating the need for control of reactive power in high PV penetration scenarios. In the rest of the discussion, we use the losses incurred in this base case to normalize the losses for the other control schemes.

B. Control on Local Voltage Only-G(V)

Controlling the $q_j^{(g)}$ on local voltage via (9) provides excellent voltage regulation with an approximate drop of 0.027 p.u. in the undergenerated case and a 0.008 p.u.

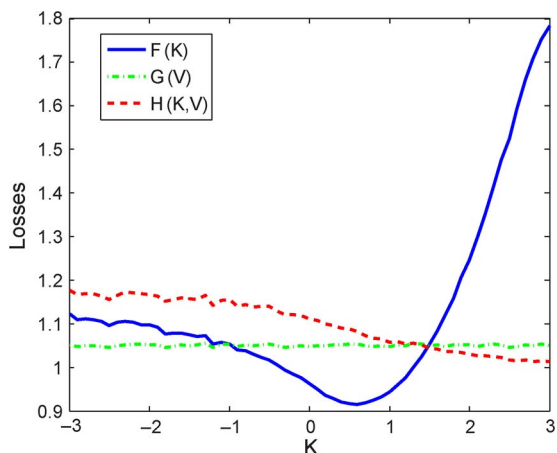


Fig. 5. Undergenerated case: Distribution circuit losses normalized by the losses when $q_j^{(g)} = 0$. Lines are the same as in Fig. 4.

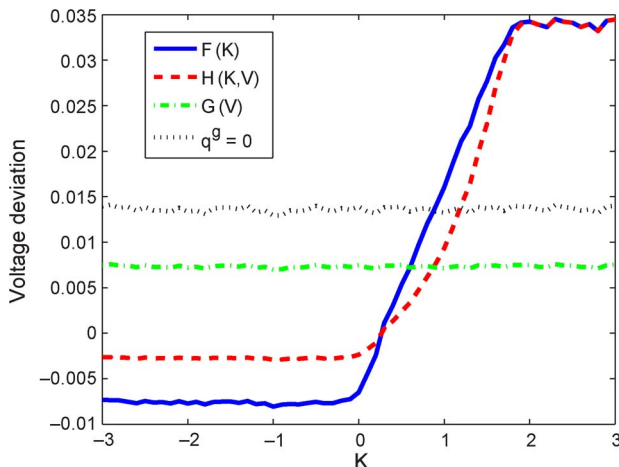


Fig. 6. Overgenerated case: maximum deviation of V_j from 1 p.u. Lines same as in Fig. 4.

rise in the overgenerated case. The total voltage swing on a partly cloudy day is reduced to about 0.035 p.u.—a significant improvement over the situation when $q_j^{(g)} = 0$. However, we note that the relative losses are increased by about 5% in the undergenerated case and by 20% in the overgenerated case. The significant increase in the overgenerated case can be traced to the rise of V_j over 1 p.u. which forces the inverters to consume reactive power increasing the flows Q_j and the dissipation. The large increase in Q_j is in part driven by our choice of $q_j^{(g)} \rightarrow \pm q_j^{\max}$ as V_j deviates significantly from 1 p.u. By reducing these limits, we could reduce the dissipation, but voltage regulation will deteriorate as the control scheme would begin to resemble $q_j^{(g)} = 0$. In a comparison of all the schemes (discussed in Section VI-E) and in Fig. 9, we show how reducing the $q_j^{(g)}$ limits impacts performance.

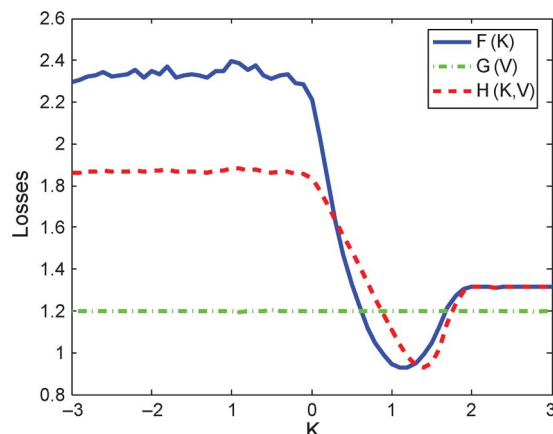


Fig. 7. Overgenerated case: Distribution circuit losses normalized by the losses when $q_j^{(g)} = 0$. Lines same as in Fig. 5.

C. Control on Local Flows Only- $F(K)$

At $K = 0$, this scheme emphasizes voltage regulation through (13). Therefore, it is not surprising that near $K = 0$ this scheme has similar voltage regulation performance as $G(V)$. Near $K = 1$ where loss reduction is emphasized via (12), $F(K)$ has significantly less dissipation than $G(V)$, but the voltage regulation is nearly as poor as $q_j^{(g)} = 0$. Clearly, there is no globally optimum value of K because, as we have discussed relative to (5) and (6), voltage regulation and loss reduction are in competition. The choice of K is then left up to engineering judgement and Fig. 9 (discussed in Section VI-E) provides a useful guide.

D. Hybrid Control- $H(K, V)$

Hybrid control via $H(K, V)$ attempts to contain large voltage deviations by smoothly switching from $F(K)$ to $G(K)$, i.e., better voltage control, as V_j move significantly away from 1 p.u. However, if V_j is close to 1 p.u., $H(K, V)$ looks more like $F(K)$ which allows for a greater emphasis on loss reduction. For both the over and undergenerated cases, the blending of $G(K)$ with $F(K)$ works well for voltage regulation with $H(K, V)$ outperforming both $G(K)$ and $F(K)$ for $K < 1$. For losses, the picture is not as clear. In the undergenerated case, $H(K, V)$ for $K < 1$ still results in increased losses over the base case and greater losses than for $G(V)$. In contrast, $H(K, V)$ for the overgenerated case results in significant loss reductions over the base case and $G(K)$ around $K = 1$. The choice of K for this control scheme is again left up to engineering judgement.

In addition to reducing losses and improving the power quality, it should be noted that the local control schemes also impact the capacity of the circuit by affecting the maximum current magnitude observed in the circuit. Fig. 8 shows potential capacity improvements (i.e., maximum current reductions) for schemes $F(K)$ and $H(K, V)$ and a capacity reduction for $G(V)$.

An assumption exploited in all our simulations is the radial structure of the network. We have assessed the importance of this assumption by running the simulations on the simple meshed network containing a single loop and found no noticeable difference in the results. This is to be expected because the distributed control schemes described in this work react to the local power flows and voltage. They are not sensitive to the global structure of the flows. Moreover, the losses and consumption of reactive power are high enough to contain the influence of reactive power injection from a single inverter to its local area.

E. Comparison of Control Schemes

Comparison of different control schemes is complicated by a conflict between the two objectives, voltage regulation and loss minimization. In this work, we are interested in finding a robust control scheme that can handle the rapid variations in power flows as a circuit with

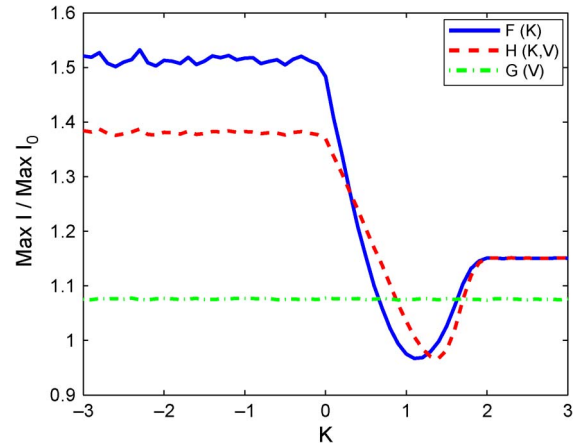


Fig. 8. Overgenerated case: Maximum current magnitude observed at any point in the circuit after the introduction of local control techniques, i.e., $(\max i) / (\max i_0)$, where i_j is the magnitude of the current flowing between the neighboring nodes in the feeder circuit, and i_0 is the magnitude of current between adjacent nodes when $q_j^{(g)} = 0$, i.e., no local injections of reactive power. Lines are the same as in Fig. 4.

a high penetration of PV undergoes rapid changes in solar irradiance. Therefore, we collapse the over and undergenerated results into a single plot by computing the maximum voltage swing experienced during the transition from over to undergenerated, i.e., the voltages in Fig. 6 minus the voltages in Fig. 4. These values make up the vertical axis in Fig. 9. To compare losses, we simply average the relative losses from Figs. 5 and 7 and these make up the horizontal axis in Fig. 9. Clearly, other ways of assessing the performance are possible. However, for this work, we choose this simple measure.

In Fig. 9, the points for $G(V)$ and $q_j^{(g)} = 0$ are two limiting points of what should be a continuous smooth curve. Indeed, as the limits defined by $q_j^{(g)}$ are decreased, the position of $G(V)$ should approach the position of $q_j^{(g)} = 0$ passing through the point labeled by $G(V)/2$ in Fig. 9 that was generated with the limits reduced by one half from the original level. The curve for the control $F(K)$ generally lies higher and to the right of the points for $G(K)$ (and its scaled versions) showing that $F(K)$ generally gives both poorer voltage regulation and higher losses. The $F(K)$ curve does fall lower and to the left of the points for $G(K)$ (and its scaled versions) for some values of K , but the voltage deviations in those cases are already approaching 0.1 p.u.

The hybrid control $H(K, V)$ and a scaled version labeled $H(K, V)/2$ (where we have reduced the upper and lower $q_j^{(g)}$ limits by a factor of 2) generally lie below and to the left of $G(K)$ and its scaled versions. The implication is that inclusion of local real and reactive power flows into a high-penetration PV inverter control scheme can lead to better performance than simply utilizing the local voltage. Plots, similar to that in Fig. 9, for other distribution

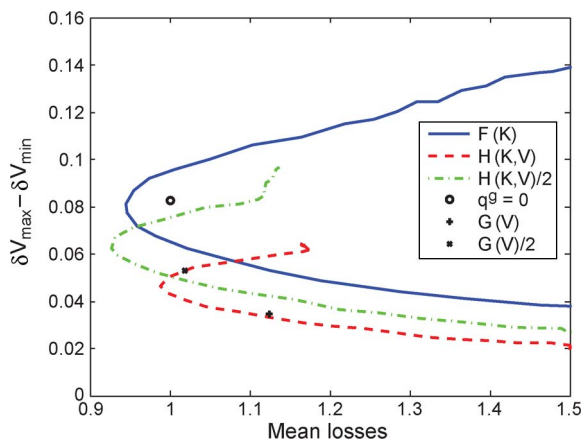


Fig. 9. Maximum per unit voltage swing experienced on the distribution circuit as the loading conditions transition from the over to undergenerated case versus the average relative losses in the over- and undergenerated cases.

circuits will clearly aid in the selection of K and the scaling factor.

In order to compare the new control schemes with a more traditional one based on capacitor banks, we have also run simulations on a modified system with one capacitor bank installed in the middle of the feeder line. Two model operation modes of a capacitor bank were analyzed. The first represents the “compensation-of-average” scheme where the bank is preprogrammed to supply a static reactive power equal to the average reactive power consumption over the feeder line. The second represents a less realistic case where we assume the capacitor bank responds dynamically, mimicking the effect of inverters by adjusting its power output to $Q(K) = \sum_j q_j(K)$, where $q_j(K)$ corresponds to the inverter’s reactive power used in $F(K)$ control scheme. Both of the cases were compared to the $F(K)$ scheme—simplest and often poorest performing of those discussed above. Although the unrealistic dynamic capacitor bank scheme performed well in reducing losses (see Fig. 10), all the distributed control schemes were superior both in terms of losses and voltage deviations. Although we did not compare the two shunt capacitor compensation schemes to the other control techniques, we expect larger gaps in performance between the $G(V)$ and $H(K,V)$ control schemes and the capacitor bank schemes.

It is difficult to compare capacitor bank control to local inverter-based control directly. We believe that our results, combined with the arguments presented in the Section III-B, indicate that the local inverter-based control solution is preferable for circuits with high penetrations of PV generation. The adjustable nature of the control schemes also makes it possible to combine the schemes, deploying smartly controlled inverters in existing power lines already using capacitor bank-based reactive compensation.

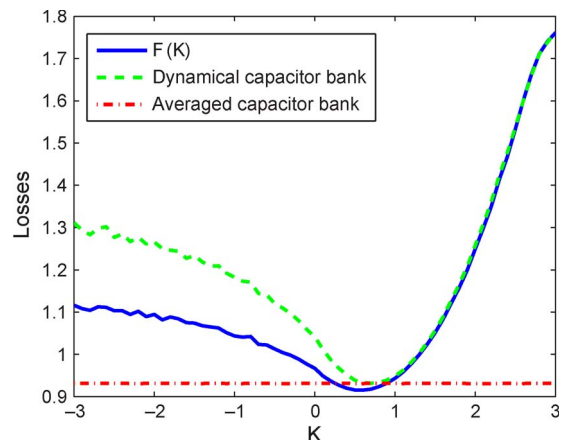


Fig. 10. Comparison of the local control scheme $F(K)$ to the traditional capacitor bank type control in the undergenerated case.

VII. CONCLUSIONS AND PATH FORWARD

We have developed and compared schemes for controlling PV inverter-generated reactive power for high PV penetration distribution circuits. In addition, we have developed a method for assessing the robustness of these and other control schemes during rapid variations in solar irradiance. Our metrics of performance included: the maximum per unit voltage change experienced during the transition from over to undergenerated conditions and the average of the dissipation for the two conditions. We have compared the control schemes developed in this work to those proposed by others [16] and have reached several conclusions:

- the fundamental competition between voltage regulation and power quality, in general, prohibits control schemes from achieving a global optimum, i.e., a minimum in voltage deviations and circuit dissipation;
- for the cases considered, control schemes that only require access to the local variables are sufficient to provide adequate voltage regulation;
- the inclusion of local real and reactive power flows, in addition to local voltage, leads to better control system performance.

In this work, we have focused mainly on the rapid transitions in loading that a high PV penetration circuit can experience during changes in solar irradiance. However, there are still open questions related to dispatch of reactive power from the PV inverters during other times. For instance, during nighttime hours when there is no PV generation and little concern about rapid changes in loading; is it equitable to use the reactive capability of the PV inverters to improve the circuit performance? If so, which control scheme (among those considered here or others) provides the best performance? We hope that this work spurs others to consider these questions in greater detail. ■

Acknowledgment

The authors are thankful to all the participants of the “Optimization and Control for Smart Grids” LDRD DR project at Los Alamos and Smart Grid Seminar Series at CNLS/LANL for multiple fruitful discussions.

REFERENCES

- [1] J. Lopes, N. Hatziaargyriou, J. Mutale, P. Djapic, and N. Jenkins, “Integrating distributed generation into electric power systems: A review of drivers, challenges and opportunities,” *Electric Power Syst. Res.*, vol. 77, no. 9, pp. 1189–1203, 2007.
- [2] A. Moreno-Munoz, *Power Quality: Mitigation Technologies in a Distributed Environment*. New York: Springer-Verlag, 2007.
- [3] *IEEE 1547 Standard for Interconnecting Distributed Resources With Electric Power Systems*. [Online]. Available: http://grouper.ieee.org/groups/scc21/1547/1547_index.html
- [4] P. Kundur, *Power System Stability and Control*. New York: McGraw-Hill, 1994.
- [5] A. Expósito, A. Conejo, and C. Cañizares, *Electric Energy Systems: Analysis and Operation*, Boca Raton, FL: CRC Press, 2008.
- [6] M. Baran and F. Wu, “Optimal sizing of capacitors placed on a radial distribution system,” *IEEE Trans. Power Delivery*, vol. 4, no. 1, pp. 735–743, Jan. 1989.
- [7] M. Baran and F. Wu, “Optimal capacitor placement on radial distribution systems,” *IEEE Trans. Power Delivery*, vol. 4, no. 1, pp. 725–734, Jan. 1989.
- [8] M. Baran and F. Wu, “Network reconfiguration in distribution systems for loss reduction and load balancing,” *IEEE Trans. Power Delivery*, vol. 4, no. 2, pp. 1401–1407, Apr. 1989.
- [9] R. Baldick and F. Wu, “Efficient integer optimization algorithms for optimal coordination of capacitors and regulators,” *IEEE Trans. Power Delivery*, vol. 5, no. 3, pp. 805–812, Aug. 1990.
- [10] T. Yona and N. Funabashi, “Optimal distribution voltage control and coordination with distributed generation,” *IEEE Trans. Power Delivery*, vol. 23, no. 2, 2008.
- [11] J. Tani and R. Yokoyama, “Coordinated allocation and control of voltage regulators based on reactive tabu search for distribution system,” *WSEAS Trans. Power Syst.*, vol. 1, no. 2, 2006.
- [12] E. Fuchs and M. Masoum, *Power Quality in Power Systems and Electrical Machines*. New York: Academic/Elsevier, 2008.
- [13] K. Turitsyn, P. Šulc, S. Backhaus, and M. Chertkov, “Use of reactive power flow for voltage stability control in radial circuit with photovoltaic generation,” *Proc. 2010 IEEE Power Eng. Soc. General Meeting*, Jul. 2010.
- [14] K. Turitsyn, P. Šulc, S. Backhaus, and M. Chertkov, “Local control of reactive power by distributed photovoltaic generators,” *Proc. 2010 IEEE SmartGridComm*, Oct. 2010.
- [15] *IEEE 1547 Standard for Interconnecting Distributed Resources With Electric Power Systems*. [Online]. Available: http://grouper.ieee.org/groups/scc21/1547/1547_index.html
- [16] B. Seal, “Standard language protocols for photovoltaics and storage grid integration,” Tech. Rep. EPRI 1020906. [Online]. Available: http://my.epri.com/portal/server.pt?Abstract_id=00000000001020906
- [17] E. Liu and J. Bebic, “Distribution system voltage performance analysis for high-penetration photovoltaics,” Tech. Rep. NREL/SR-581-42298. [Online]. Available: <http://www1.eere.energy.gov/solar/pdfs/42298.pdf>
- [18] K. Schneider, Y. Chen, D. Chassin, R. Pratt, D. Engel, and S. Thompson, “Modern grid initiative-distribution taxonomy final report,” Tech. Rep. [Online]. Available: http://www.gridlabd.org/models/feeders/taxonomy_of_prototypical_feeders.pdf
- [19] P. Kundur, *Power Systems Stability Control*. New York: McGraw-Hill, 1993.

ABOUT THE AUTHORS

Konstantin Turitsyn (Member, IEEE) received the M.Sc. degree in physics from Moscow Institute of Physics and Technology and the Ph.D. degree in physics from Landau Institute for Theoretical Physics, Moscow, in 2007.

Currently, he is an Assistant Professor at the Mechanical Engineering Department at Massachusetts Institute of Technology (MIT), Cambridge. Before joining MIT, he held the position of Oppenheimer fellow at Los Alamos National Laboratory, and Kadanoff-Rice Postdoctoral Scholar at University of Chicago. His research interests encompass a broad range of problems involving nonlinear and stochastic dynamics of complex systems. Specific interests in energy related fields include statistical models of renewable generation, distributed control of energy delivery systems, and dynamics of large scale power grids.



Petr Šulc received the Master’s degree in mathematical physics at the Faculty of Nuclear Sciences and Physical Engineering at Czech Technical University, Prague, Czech Republic, in 2009 and the Master’s degree in quantum physics at Ecole Polytechnique, Palaiseau, France, in 2009. He is currently working towards the Ph.D. degree at the Rudolf Peierls Centre for Theoretical Physics, University of Oxford.

From 2008 to 2009, he worked as a research intern studying applications of statistical physics to complex system at the LPTMS, University Paris-Sud, Orsay, France. From August 2009 to August 2010, he was a graduate research assistant working on optimization problems in CNLS, Los Alamos National Laboratory and New Mexico Consortium.



Scott Backhaus received the Ph.D. degree in physics from the University of California at Berkeley in 1997 in the area of experimental macroscopic quantum behavior of superfluid He-3 and He-4.

In 1998, he came to Los Alamos, NM, was Director’s Funded Postdoctoral Researcher from 1998 to 2000, a Reines Postdoctoral Fellow from 2001 to 2003, and a Technical Staff Member from 2003 to the present. While at Los Alamos, he has performed both experimental and theoretical research in the area of thermoacoustic energy conversion for which he received an R&D 100 award in 1999 and *Technology Review’s* “Top 100 Innovators Under 35” award in 2003. Recently, his attention has shifted to other energy-related topics including the fundamental science of geologic carbon sequestration and grid-integration of renewable generation.

Michael Chertkov received the Ph.D. degree in physics from the Weizmann Institute of Science, Rehovot, Israel, in 1996, and the M.Sc. degree in physics from Novosibirsk State University, Russia, in 1990.

After receiving the Ph.D. degree, he spent three years at Princeton University, Princeton, NJ, as an R.H. Dicke Fellow in the Department of Physics. He joined Los Alamos National Lab in 1999, initially as a J. R. Oppenheimer Fellow in the Theoretical Division. He is now a Technical Staff Member in the same division. He has published more than 100 papers in these research areas and is currently leading “Physics of Algorithms” and “Optimization and Control Theory for Smart (Power) Grids” projects at LANL. His areas of interest include applied and theoretical problems in power systems, hydrodynamics, statistical and mathematical physics, information theory, and computer science.

